Virology 378 (2008) 21–33

Contents lists available at ScienceDirect

Virology

journal homepage: www.elsevier.com/locate/yviro

Lymphocytic choriomeningitis virus uses a novel endocytic pathway for infectious entry via late endosomes

Katharina Quirin [a], Bruno Eschli [b], Isabella Scheu [a], Linda Poort [a], Jürgen Kartenbeck [c], Ari Helenius [a,*]

[a] Institute of Biochemistry, ETH Zurich, Schafmattstrasse 18, CH-8093 Zurich, Switzerland
[b] Institute of Experimental Immunology, University Hospital Zurich, Schmelzbergstrasse 12, CH-8091 Zurich, Switzerland
[c] Division of Cell Biology, German Cancer Research Center (DKFZ), D-69120 Heidelberg, Germany

ARTICLE INFO

Article history:
Received 23 January 2008
Returned to author for revision
22 February 2008
Accepted 28 April 2008
Available online 13 June 2008

Keywords:
Virus entry endocytosis
Clathrin
Lipid rafts
Endosomes

ABSTRACT

The endocytic entry of lymphocytic choriomeningitis virus (LCMV) into host cells was compared to the entry of viruses known to exploit clathrin or caveolae/raft-dependent pathways. Pharmacological inhibitors, expression of pathway-specific dominant-negative constructs, and siRNA silencing of clathrin together with electron and light microscopy provided evidence that although a minority population followed a classical clathrin-mediated mechanism of entry, the majority of these enveloped RNA viruses used a novel endocytic route to late endosomes. The pathway was clathrin, dynamin-2, actin, Arf6, flotillin-1, caveolae, and lipid raft independent but required membrane cholesterol. Unaffected by perturbation of Rab5 or Rab7 and apparently without passing through Rab5/EEA1-positive early endosomes, the viruses reached late endosomes and underwent acid-induced penetration. This membrane trafficking route between the plasma membrane and late endosomes may function in the turnover of a select group of surface glycoproteins such as the dystroglycan complex, which serves as the receptor of LCMV.

Introduction

Many animal viruses exploit the endocytic machinery of their host cells for infectious entry (Marsh and Helenius, 2006). After receptor binding, they are internalized and transported in endocytic vesicles to intracellular organelles from which they escape into the cytosol and infect the cell. A large number of viruses, including Semliki Forest virus (SFV), have been shown to make use of the classical clathrin-mediated pathway to reach endosomes where the low pH triggers penetration (Helenius et al., 1980). According to their pH-threshold of activation, these viruses penetrate from either early (pH 6.5–6.0) or late endosomes (pH 6.0–5.0) (Kielian et al., 1986). Other viruses, such as Simian virus 40 (SV40), are known to use alternative, pH-neutral, caveolae/lipid-raft-mediated pathways that carry them to caveosomes and the ER for penetration (Parton and Richards, 2003). That viruses have evolved to use distinct endocytic processes has made them valuable as tools for characterizing the complex endocytic capabilities of mammalian cells.

In this study, we have focused on lymphocytic choriomeningitis virus (LCMV), an enveloped, negative-stranded RNA virus of the arenavirus family. LCMV persistently infects mice and can be transmitted from these to humans, causing aseptic meningitis (Peters, 2006). Congenital LCMV infection is considered an under-diagnosed human fetal teratogen (Barton and Mets, 2001). In addition to LCMV, the arenavirus family comprises emerging pathogens such as Junin, Machupo, Lassa, Guanarito, and Sabia viruses, which all cause severe hemorrhagic fevers when transmitted to humans (Charrel and Lamballerie, 2003).

Like other arenaviruses, LCMV particles are pleomorphic in appearance. They have a mean diameter of 86±21 nm, and they are roughly spherical with spike-like projections formed by the envelope glycoproteins (Neuman et al., 2005). The glycoproteins are trimeric class I membrane fusion proteins, composed of fusion-mediating transmembrane subunits (GP-2) associated with receptor-binding subunits, GP-1 (Buchmeier, 2002; Eschli et al., 2006).

The major receptor for LCMV and other Old World arenaviruses has been identified as α-dystroglycan, a highly glycosylated, peripheral plasma membrane protein with affinity for components of the extracellular matrix (Cao et al., 1998). Receptor binding involves lectin-like recognition of glycans on α-dystroglycan (Imperiali et al., 2005; Kunz et al., 2004, 2005). Previous studies have established that LCMV belongs to the acid-activated viruses: the virus is inactivated by incubation in mildly acidic buffers, and fusion of LCMV with liposomes is induced by reduced pH (Di Simone and Buchmeier, 1995, 1994). Furthermore, drugs interfering with organelle acidification inhibit infection (Borrow and Oldstone, 1994; Di Simone et al., 1994). After escaping from an unidentified organelle by acid-induced membrane fusion, LCMV replicates in the cytosol.

Our interest in LCMV was triggered by electron micrographs that showed the incoming virus in smooth-walled pits in the plasma

* Corresponding author. Institute of Biochemistry, ETH Zurich, Schafmattstrasse 18, CH-8093 Zurich, Switzerland. Fax: +41 44 632 1269.
E-mail address: ari.helenius@bc.biol.ethz.ch (A. Helenius).

0042-6822/$ – see front matter © 2008 Elsevier Inc. All rights reserved.
doi:10.1016/j.virol.2008.04.046

membrane, suggesting an entry pathway independent of clathrin coats (Borrow and Oldstone, 1994). By comparing the requirements for LCMV infection with those for SFV and SV40, by silencing clathrin genes, and by analyzing the process of infectious entry using a variety of inhibitors and dominant-negative (DN) constructs, we analyzed the entry route of LCMV in more detail.

Results

LCMV in smooth and coated structures by electron microscopy

To investigate the morphology of LCMV uptake, an inoculum of strain LCMV-WE was added to Vero cells on ice, and the cell-bound viruses were immunolabeled with 10 nm gold particles. After internalization for different periods at 37 °C, the cells were fixed and prepared for transmission electron microscopy. As described previously for the strain LCMV clone 13 (Borrow and Oldstone, 1994), entry was asynchronous. Consistent with published images of LCMV clone 13 (Borrow and Oldstone, 1994), we observed gold-labeled LCMV-WE particles closely bound to smooth segments of the plasma membrane, in smooth-walled invaginations of the plasma membrane, and close to the plasma membrane in structures that may represent primary endocytic vesicles (Fig. 1A). LCMV inside cytoplasmic vesicles and larger sometimes multivesicular vacuoles represented later steps of the entry process (Figs. 1C and D). However, LCMV-WE particles could also occasionally be seen in clathrin-coated structures (Fig. 1B, compare smooth and coated structures on the left and right panels). This raised the possibility of the virus utilizing two endocytic pathways: a clathrin-mediated and an uncoated pathway of endocytosis.

Infection is clathrin independent

To address the involvement of clathrin-mediated endocytosis (CME) in LCMV-WE infection, we depleted HeLa cells of clathrin heavy chain (CHC) using two different, non-overlapping siRNAs in parallel experiments. With each siRNA, the protein level of CHC in the cultures was reduced by 80–90% as assayed by Western blotting (Fig. 2A). By immunofluorescence microscopy, a large fraction of the cells were devoid of CHC staining on the plasma membrane although some intracellular staining could be seen (Fig. 2B). The majority of cells were unable to take up transferrin (Fig. 2B, arrow heads), while a few still accumulated intracellular transferrin (asterisks). We focused on the cells incapable of internalizing transferrin and found, using immunostaining for the nucleoprotein (NP) of LCMV, that these cells were efficiently infected (Fig. 2B, quantification Fig. 2C). In contrast, infection with Semliki Forest virus, which uses the clathrin pathway exclusively, was strongly inhibited in these cells (Figs. 2B and C). Control cells transfected with an unrelated siRNA took up transferrin and were infected normally by both viruses.

These results demonstrated that contrary to SFV, LCMV does not require CME for productive infection of host cells. Thus, the smooth vesicles observed by electron microscopy were apparently able to support productive entry of the virus. The partial decrease in LCMV infectivity in clathrin depleted cells was, however, consistent with the possibility that a minority fraction of viruses did make use of CME for infectious entry.

We also probed the influence of DN proteins commonly used to inhibit CME. Eps15, an accessory protein, binds to the adaptor protein complex AP-2. Expression of the deletion mutant Eps15 Δ95-295 interferes with AP-2 recruitment to the plasma membrane, impedes the assembly of clathrin-coated pits, and prevents the endocytosis of transferrin (Benmerah et al., 1999, 1998). AP180 is the neuronal isoform of CALM, the ubiquitously expressed clathrin assembly lymphoid myeloid leukemia protein thought to play a regulatory role in clathrin coat formation (Meyerholz et al., 2005). Overexpression of full-length or truncated AP180/CALM inhibits endocytosis of EGF and transferrin

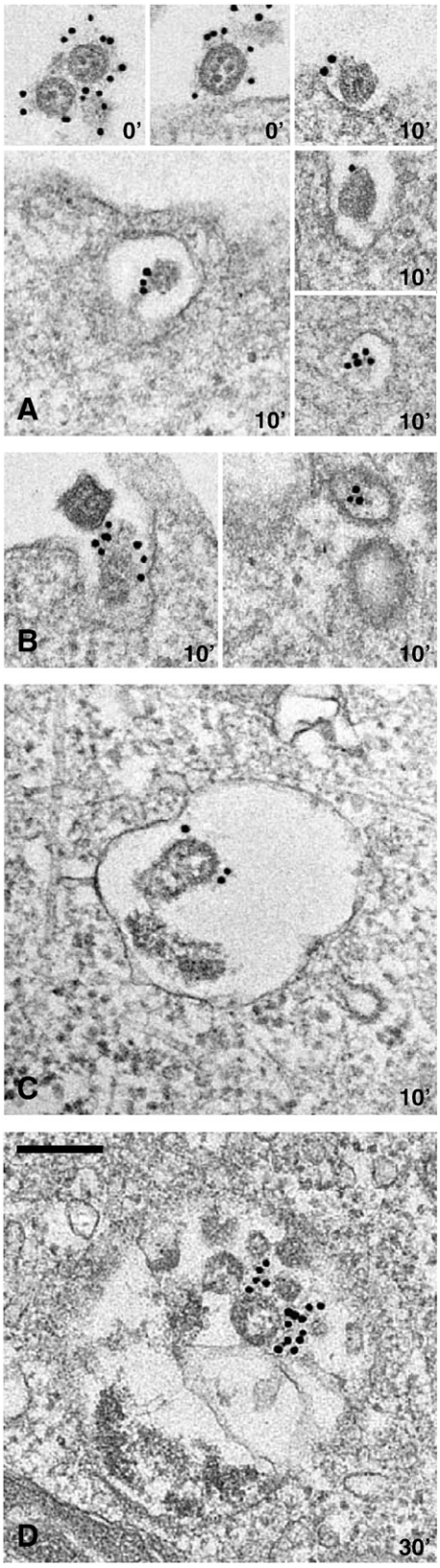

Fig. 1. Electron microscopy on LCMV entry. LCMV inoculum was added to Vero cells for 1 h on ice and unbound virus washed away. The cell-bound viruses were immunolabeled with 10 nm gold particles and allowed to enter the cells at 37 °C for 0 min (A, upper left and middle panels), 10 min (A large panel and right column, B, C), or 30 min (D). The virus was efficiently labeled (A, upper left panel showing free LCMV particles) and was observable in smooth and clathrin-coated structures of the host cell's plasma membrane (A, B), as well as in intracellular vesicles and vacuoles (C, D). Of the vacuoles, some were multivesicular (D). Scale bar: 200 nm.

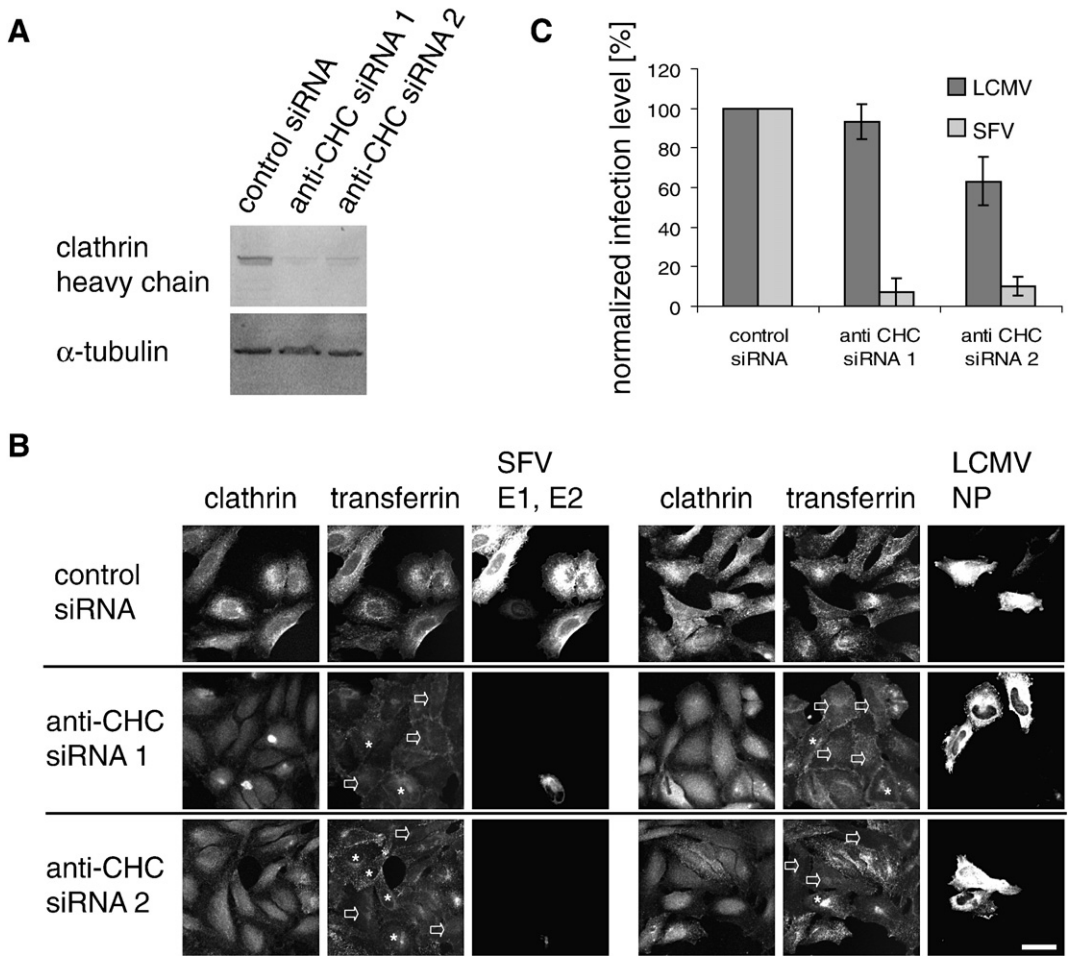

Fig. 2. LCMV infection is independent of clathrin. The CHC gene was silenced in HeLa cells using transfection with two different siRNAs, and the effect on LCMV and SFV infection was determined. (A) Efficiency of clathrin heavy chain knockdown was assayed by Western blotting. (B) HeLa cells transfected with control or anti-CHC-siRNAs were infected with LCMV or SFV (MOI ≤ 0.5) and incubated with fluorescently labeled transferrin. Immunostaining against clathrin confirmed reduced CHC levels. Transferrin uptake was found to be fully blocked in a subpopulation of clathrin depleted cells (arrows), while other cells still accumulated transferrin (asterisks). LCMV infection occurred in both cell types, as detected by staining against the viral NP. SFV infection was detected by immunostaining against envelope proteins and was strongly inhibited in the CME deficient cells. Scale bar: 40 μm. (C) Quantification of panel B. The level of infection in cells incapable of transferrin uptake was normalized to the infection level in cells transfected with control siRNA. The absolute infection level in the control samples was 20–50% for both viruses. Per virus and siRNA, three times 200 cells were counted in two independent experiments, error bars: SD.

by interfering with clathrin-coated pit formation (Ford et al., 2001; Tebar et al., 1999).

To confirm the effect of Eps 15 and AP180 on CME in our experiments, DN or control constructs were transiently expressed in Vero cells as EGFP fusion proteins, and transferrin uptake was assayed by microscopy. As expected, expression of the DN proteins, but not of controls, inhibited transferrin uptake. However, the inhibition by AP180 was only partial in some cells (Fig. 3A, asterisk). In parallel, virus infection was assayed after addition of LCMV or SFV at low multiplicity (MOI ~0.5) by immunostaining for newly synthesized LCMV NP or SFV E1 and E2, respectively. Flow cytometry was used here and in subsequent experiments to quantify the intensity of the viral staining and the EGFP signal, with no crosstalk between the channels (Fig. 3C, panels 1–3). To assess the effect of a given DN protein rigorously and quantitatively, we defined for each sample in the histogram of the EGFP signal a "non-expressing" cell population that was negative for EFGP-fusion protein and an "expressing" cell population containing high levels of the protein. This is illustrated in Fig. 3C (panels 4 and 7) using dynamin-2 K44A-EGFP. The infection level within each population was quantified in a histogram of the virus staining intensity (Fig. 3C, panels 5 and 6 for LMV; panels 8 and 9 for SFV). To control for fluctuations in cell number, we defined the relative infection level as the percentage of infected cells in the "expressing" cell population divided by the percentage of infected cells in the "non-expressing" cell population. Absolute infection levels in non-transfected control cells were 30–60%. LCMV infection was inhibited by only 20% (DN Eps15) and 5% (DN AP180) consistent with a major clathrin-independent mechanism of LCMV endocytosis also in Vero cells (Fig. 3B). However, the DN constructs had only a partial inhibitory effect on SFV. Since SFV infection strictly relies on CME, the results suggested that SFV can make use of a clathrin-mediated pathway that is independent of eps15. The apparent lack of AP2 dependence implied by this result is not unprecedented among CME cargo (Conner and Schmid, 2003; Hinrichsen et al., 2003; Lakadamyaliet al., 2006; Motley et al., 2003). The partial effect of AP180 on SFV infection probably reflects the "leakiness" of this inhibition protocol, as reflected by the partial inhibition of transferrin uptake (cf. Fig. 3A, asterisk).

Infection is dynamin-2 independent

The large GTPase dynamin-2 is involved in pinching off clathrin-coated vesicles, caveolae, and certain types of lipid-raft-dependent vesicles from the plasma membrane. Expression of DN dynamin mutants inhibits these forms of endocytosis (Lamaze et al., 2001; Oh et al., 1998; Sauvonnet et al., 2005; van der Bliek et al., 1993).

Dynamin-2 wild-type and the DN mutant dynamin-2 K44A were transiently expressed as EGFP fusion proteins and the cells were infected with LCMV or SFV at low multiplicity (MOI ≤ 0.5). The fraction of cells expressing a given fusion protein was determined by flow cytometry as described above (Fig. 3C). As expected, dynamin-2 K44A expression reduced SFV infection by 80%, but expression of wild-type dynamin-2 had little effect in either Vero or HeLa cells (Figs. 3D and E). In line with a clathrin-independent major entry route, LCMV infection did not depend on dynamin-2 activity in either cell line. This finding was not only consistent with the non-involvement of CME as a major

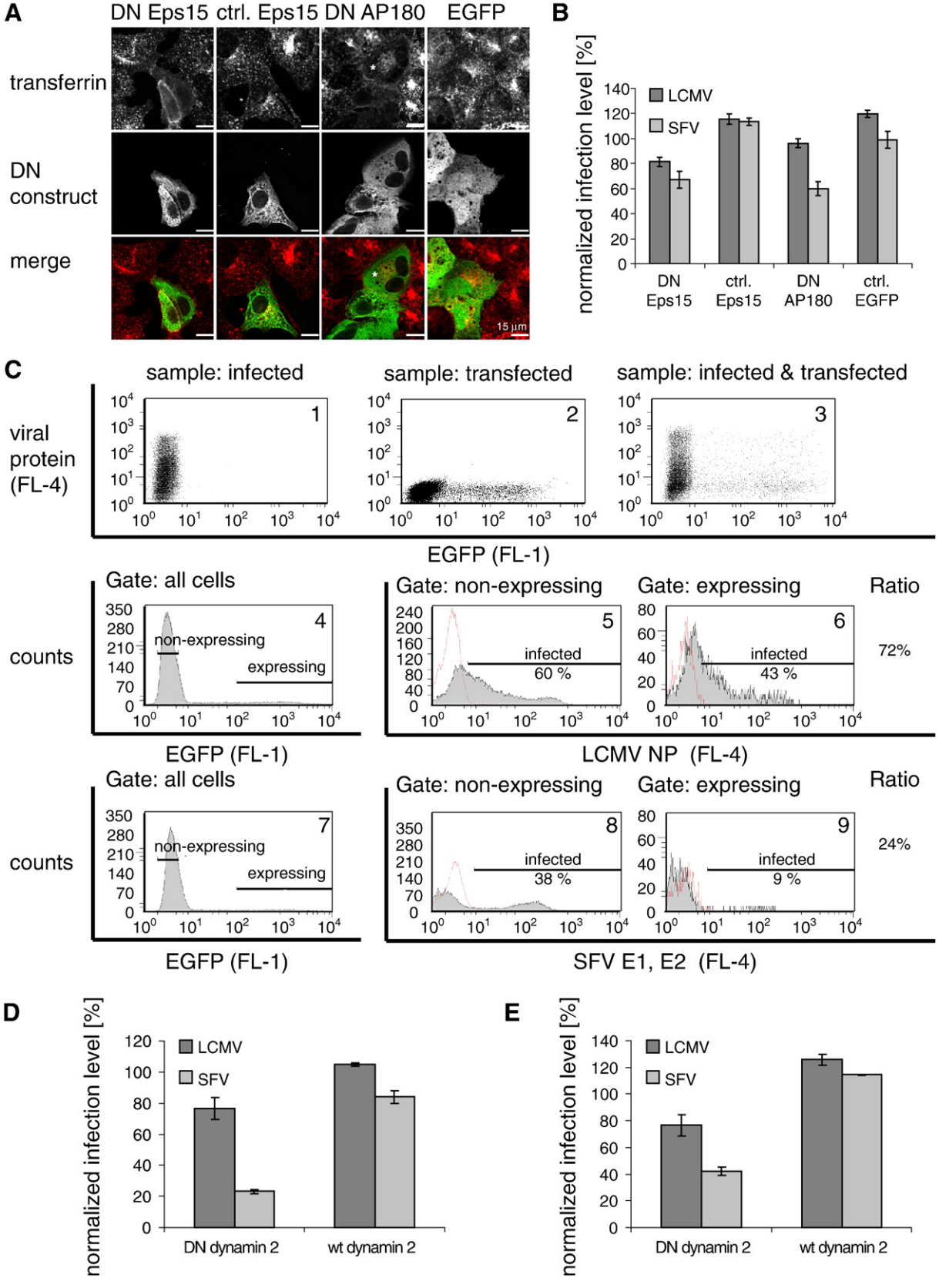

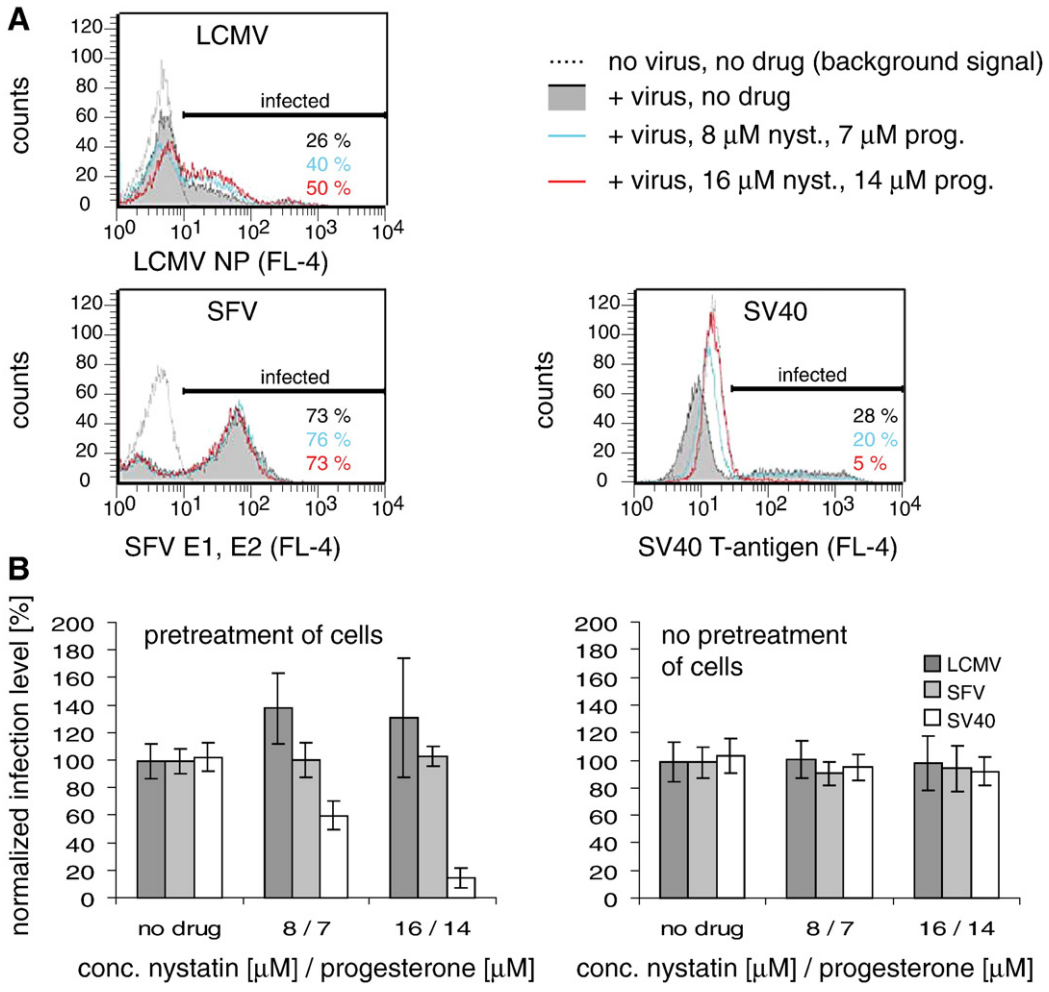

Fig. 4. LCMV infection is slightly enhanced upon mild cholesterol depletion. (A) Histograms of virus staining intensity before and after cholesterol depletion. (B) Left: Vero cells pre treated with nystatin/progesterone were infected with SV40, LCMV, or SFV in the continued presence of the drugs. For LCMV, the drugs were replaced 180 min p.i. by NH_4Cl containing medium to block further penetration of the virus. The infection level was determined by immunostaining of viral proteins and flow cytometry and was normalized to samples where the inhibitors had been omitted. Right: Vero cells were infected in the presence of nystatin/progesterone as left, but the drugs were only present during incubation of cells with inocula. Data shown are averages ± SD of three independent experiments, each with triplicate samples. MOI ~0.5 for all viruses.

pathway of entry, but it also ruled out caveolar endocytosis and some of the other lipid-raft-mediated pathways in LCMV infection. However, since not all lipid-raft-mediated pathways are dynamin-2 dependent (see, e.g., Damm et al., 2005; Sabharanjak et al., 2002), we next adressed the potential involvement of lipid rafts in LCMV infection more directly.

LCMV infection is lipid raft independent

The caveolae/raft-dependent pathways are highly sensitive to cholesterol-depleting agents, whereas CME is only affected at high doses (Anderson et al., 1996; Damm et al., 2005; Subtil et al., 1999). To probe whether any step in LCMV entry prior to the pH-induced penetration in acidic organelles was sensitive to perturbation of lipid rafts, we preincubated cells with increasing concentrations of nystatin and progesterone. The cells were then infected with LCMV, SV40 (positive control: a virus that uses caveolae/raft pathways), or SFV (negative control: a virus that uses CME) in the continued presence of these inhibitors. The inhibitors were washed out 180 min post-infection (p.i.) and replaced by the lysosomotropic agent NH_4Cl to prevent further penetration. As a membrane permeable weak base, NH_4Cl raises the endosomal pH nearly instantaneously (Ohkuma and Poole, 1978) and thereby intercepts any incoming viruses that have not yet undergone the acid-induced membrane fusion step (Borrow and Oldstone, 1994). Since NH_4Cl is not toxic to cells, we could in this way ensure better viability of the cells during the infection period.

Fig. 3. LCMV infection is not affected by DN Eps15, DN AP180, or DN dynamin-2. (A) Transferrin uptake in Vero cells transiently transfected with Eps15-EGFP, AP180-EGFP, or control constructs. Expression of the DN, but not the control constructs, inhibited transferrin uptake. Inhibition by AP180 was partial in some cells (asterisk). (B) Effect of DN Eps15 and AP180 overexpression on SFV and LCMV infection, quantified by flow cytometry. Data shown are averages of triplicate samples ± SD. (C) Assay setup to determine the effect of DN proteins on virus infection by flow cytometry. The EGFP fusion protein of interest (shown here: dynamin-2 K44A) was transiently expressed in Vero cells, the cells were infected with LCMV or SFV (MOI ~0.5), and infection was detected by immunostaining against viral proteins. The EGFP signal used to quantify the expression level of the DN protein and the fluorescent staining of viral protein were detected independently with no crosstalk between the channels (panels 1–3). Panels 4–6 show histograms of EGFP and virus staining intensities for an LCMV infected sample; panels 7–9 show the same for an SFV infected sample. Two populations of cells were selected in each sample based on predefined intensity ranges of the EGFP signal: A "non-expressing" population negative for EGFP and an "expressing" population containing high levels of the construct. The percentage of cells infected within each population was quantified in a histogram of the virus staining intensity (panels 5, 6 and 8, 9), using non-infected stained control samples (red traces) to define the threshold of virus staining intensity above which a cell was infected. The effect of a given EGFP-fusion protein was expressed as normalized infection level, i.e., the ratio of the infection level in the cell population expressing the protein divided by the infection level in the non-expressing cell population. (D) Effect of dynamin-2 wt and K44A overexpression on SFV and LCMV infection in Vero cells or (E) HeLa cells, quantified by flow cytometry. Data shown are averages of triplicate samples ± SD. MOI ~0.5 for all viruses.

As expected, SV40 infection was inhibited by cholesterol depletion and sequestration in a dose-dependent manner, while SFV infection was not affected (Fig. 4B, left). That SV40 was inhibited indicated that functional lipid-rafts were destroyed, while the lack of effect on SFV infection indicated that the CME was functional and that early endosomes still contained enough cholesterol to support SFV fusion, a cholesterol-dependent process (Phalen and Kielian, 1991). In contrast, LCMV infection was slightly increased. If preincubation of the cells was omitted and the cholesterol-depleting agents were added to the inoculum only, no enhancement of LCMV infection could be detected (Fig. 4B, right). Thus, the increase in LCMV infection was due to cholesterol depletion of cellular membranes; i.e., it was not caused by modifications of the viral envelope. We concluded that unlike SV40, LCMV was not entering cells via pathways that required the presence of lipid rafts. This was consistent with a caveolin-independent mechanism.

Flotillin-1 and Arf6 independence of LCMV infection

A recent study has demonstrated that the lipid-raft-associated protein flotillin-1 is internalized with fluid phase markers, GPI-anchored GFP and cholera toxin, and colocalizes with these in endosomal structures. The process is flotillin-1 dependent and independent of clathrin, and a connection with lipid-raft-mediated pathways appears likely (Glebov et al., 2006). In order to address a potential involvement of flotillin-1 in LCMV entry, we investigated whether incoming LCMV colocalizes with endogenous flotillin-1 at early time points of infection. Vero cells were treated at 4 °C with LCMV (MOI ~50), warmed to 37 °C, incubated for different times, and fixed for immunostaining. Confocal fluorescence microscopy was used to localize the virus and to quantify its colocalization with marker proteins using stringent, quantitative colocalization criteria (see Materials and methods). The fraction of viruses colocalizing with flotillin-1 at 2, 5, and 10 min post-warming was very low (Fig. 5).

Since the level of colocalization was comparable to that observed with a negative control (the subunit γ of COP-I, see Fig. 8C), it probably reflected the background. We concluded that flotillin-1 was unlikely to be involved in LCMV entry.

The small GTPase Arf6 localizes to the plasma membrane and to endosomal membranes, where it is involved in a variety of endocytic processes (D'Souza-Schorey and Chavrier, 2006; Donaldson, 2003). In its active, GTP-bound state, Arf6 can stimulate $PI(4,5)P_2$ formation, and it is involved in clathrin-coated pit formation (Krauss et al., 2003; Paleotti et al., 2005). Furthermore, Arf6 has been reported to stimulate lipid-raft-dependent traffic of MHC I and of the GPI-anchored protein CD59 to a distinct, Arf6-positive endosome in HeLa cells. The Arf6 compartment accumulates cargo molecules and fluid phase markers and is at early time points (2 min) distinct from the CME pathway. Later, both pathways merge at the early endosome (Naslavsky et al., 2003; Naslavsky et al., 2004).

To address a potential role of Arf6 in LCMV endocytosis, we examined the effect of overexpression of a wild-type Arf6 and a constitutively inactive, GDP-bound mutant form (Arf6 T27N) on LCMV infection. Neither protein had any effect suggesting that LCMV entry is not dependent on or regulated by Arf6 activation (Fig. 6A). We also could not observe significant colocalization between LCMV and transiently expressed wild-type Arf6-EGFP by confocal microscopy (Fig. 6B).

LCMV infection is independent of macropinocytosis

To address a potential involvement of macropinocytosis, we assessed the sensitivity of LCMV infection to cytochalasin D, jasplakinolide, and amiloride. These agents inhibit macropinocytosis by inhibiting actin polymerization or Na^+/H^+ exchange at the plasma membrane (Swanson and Watts, 1995). By replacing the inhibitor of interest against NH_4Cl 3 h after initial infection as described above, we focused again on inhibitory effects that the inhibitors might have in the early steps of LCMV uptake and traffic.

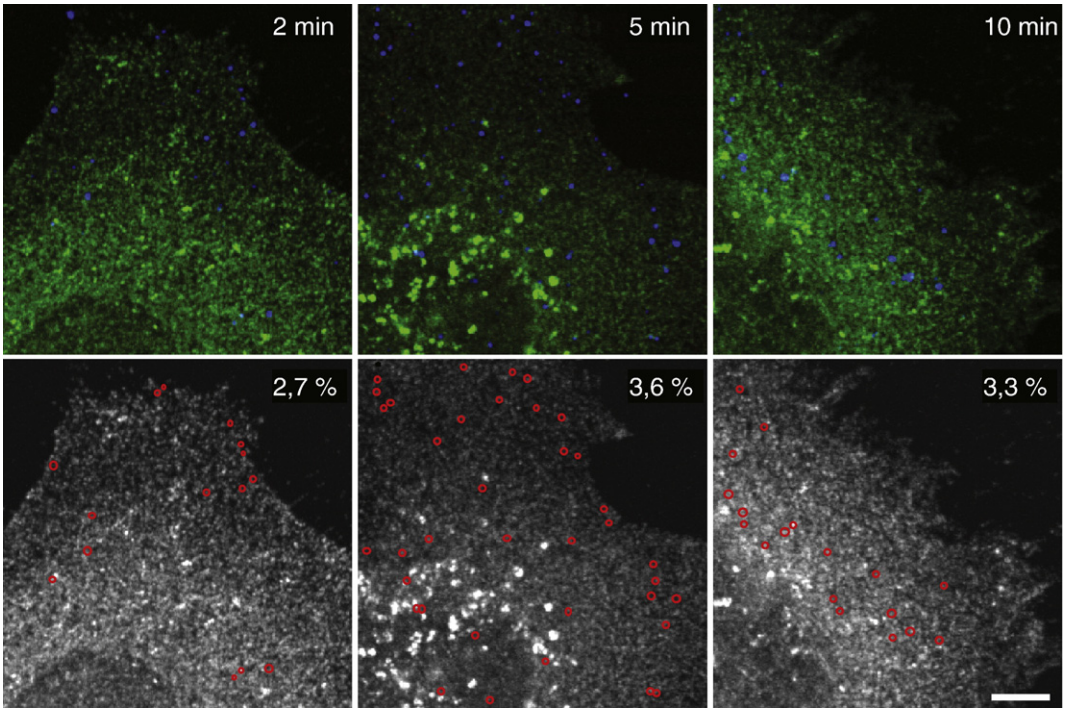

Fig. 5. LCMV infection is independent of Flotillin-1. Entry of pre-bound LCMV into Vero cells by confocal microscopy. Top: LCMV in blue; endogenous, immunostained Flotillin-1 in green. Bottom: same micrographs of flotillin-1 as above, position of LCMV particles indicated by hollow circles to facilitate the colocalization analysis. Percentages of colocalization were determined by counting 200 virus particles in 3–5 cells per time point. Scale bar: 5 μm.

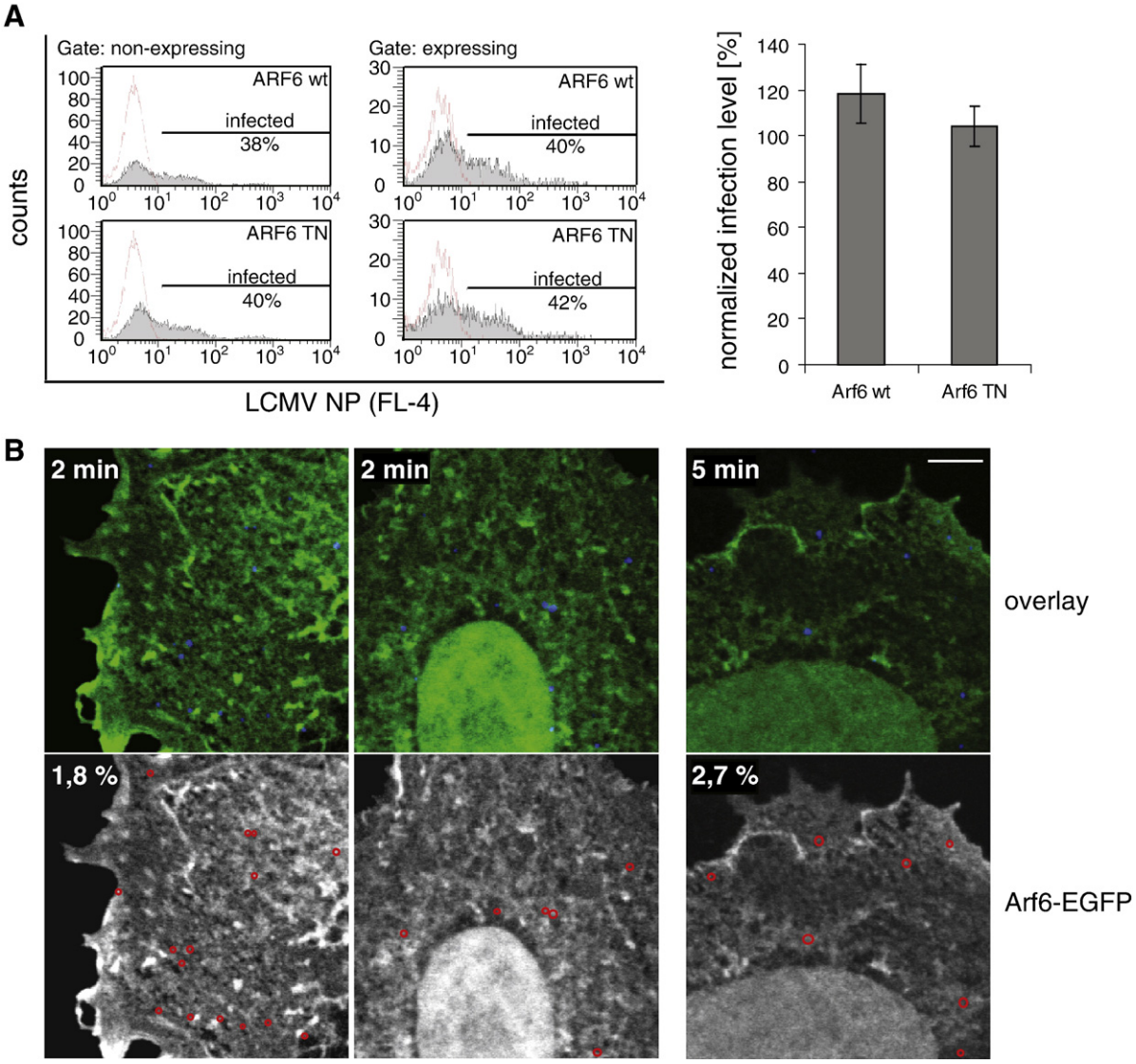

Fig. 6. LCMV infection is independent of Arf 6. (A) Influence of expression of EGFP-labeled Arf-6 wt and Arf-6 T27N assayed by FACS analogous to Fig. 3C (MOI ~0.5). For both proteins, the infection level was the virtually the same in the subpopulation expressing the protein as compared to the non-expressing control cells within the same sample. (B) Entry of pre-bound LCMV into Vero cells expressing EGFP-labeled Arf-6 wt by confocal microscopy. Top: LCMV in blue; EGFP-labeled Arf-6 wt in green. Bottom: same micrographs of Arf6 signal as above, position of LCMV particles indicated by hollow circles to facilitate the colocalization analysis. Percentages of colocalization were determined by counting 200 virus particles in 3–5 cells per time point. Scale bar: 5 μm.

LCMV-WE infection was not affected by amiloride treatment (Fig. 7A). Instead of inhibiting, the F-actin depolymerizing agent cytochalasin D and the F-actin stabilizing agent jasplakinolide caused a clear increase in infection (Fig. 7A). This effect was likely caused by the disruption of the cortical actin meshwork, an effect that could be observed with both drugs (Fig. 7B). In line with this, we also observed a pronounced increase in LCMV infection upon treatment with the F-actin depolymerizing agent latrunculin A (data not shown). It is possible that the cortical actin meshwork impedes LCMV entry by constituting a physical barrier for vesicle movement or by immobilizing factors needed for LCMV endocytosis. Further, changes in cell shape upon drug treatment might lead to shortening of the distance between the plasma membrane and late endosomes, hence facilitating infection. Taken together, the data indicated that LCMV-WE was not infecting cells via macropinocytosis, which is consistent with previous data on LCMV clone 13 (Borrow and Oldstone, 1994). In addition, the lack of inhibition by jasplakinolide and latrunculin A was in marked contrast to the requirements reported for caveolar entry of SV40 (Pelkmans et al., 2002).

LCMV reaches late endosomes but bypasses early endosomes

Next, we asked to which acidic organelles LCMV was transported inside the cell and where was the acid-induced penetration taking place. First, we determined the kinetics of LCMV penetration using a protocol previously employed for SFV (Helenius et al., 1980). Virus was bound to cells on ice at low multiplicity (MOI<0.2), unbound virus was washed off, after which the cells were rapidly warmed and incubated for different time intervals at 37 °C before addition of NH_4Cl containing medium to block further penetration. As a benchmark, we determined the penetration kinetics of two SFV strains that enter cells via CME but have different pH thresholds for fusion. Wild-type SFV penetrates at pH<6.2 in early endosomes, while the SFV fus-1 mutant does so at pH<5.5 in late endosomes (Kielian et al., 1986). LCMV penetration occurred within 10–30 min post-warming with a half time of 16.4 min±2.1 min, compared to 6.2 min for wild-type SFV and 14.2 min for the mutant SFV fus-1 (Fig. 8A). With respect to the time course of penetration, LCMV thus resembled fus-1.

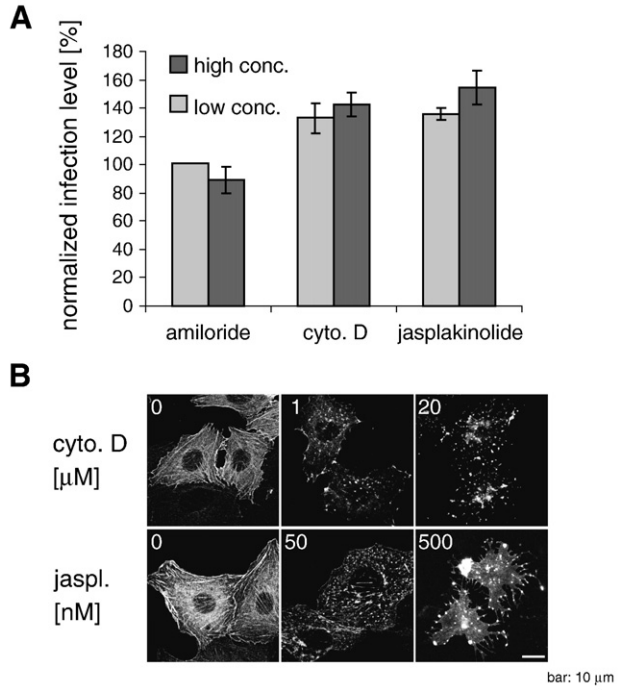

Fig. 7. LCMV infection is independent of macropinocytosis. (A) Vero cells pre-treated with amiloride (1, 20 μM), cytochalasin D (1, 20 μM), or jasplakinolide (50, 500 nM) were infected with LCMV in the continued presence of the inhibitors. The drugs were replaced 180 min p.i. by NH_4Cl containing medium to block further penetration of the virus. The infection level was determined by immunostaining of viral proteins and flow cytometry and was normalized to samples where the drugs had been omitted. Error bars: SD of triplicate samples. (B) Vero cells expressing EGFP actin show a disrupted cortical actin cytoskeleton after treatment with jasplakinolide or cytochalasin D.

To determine whether LCMV entered early or late endosomes, Vero cells expressing the early endosome marker Rab5-EGFP or the late endosome marker Rab7-EGFP were treated with LCMV (MOI ~50), warmed to 37 °C, incubated for different time intervals, and fixed for immunostaining of LCMV using anti-NP. As before, confocal fluorescence microscopy was used to visualize the virus and to quantify its colocalization with marker proteins using stringent, quantitative criteria (Figs. 8B and C; see Methods section). As a negative control, we used colocalization with the immunostained subunit γ of COP I and found that it did not exceed 3%.

Colocalization of LCMV with Rab5-EGFP exhibited a maximum of 10% at 5 min post-warming (Fig. 8C), decreasing rapidly thereafter to background values within 40 min post-warming. In contrast, colocalization of LCMV with Rab7-EGFP reached 15% within 20 min post-warming and remained high (Fig. 8C). Similar colocalization time courses were observed in HeLa cells for Rab5 and Rab7 (Fig. S1), as well as for the endogenous markers EEA1 and LAMP-1 (Figs. 8E and F, hatched lines) and transferrin (a contents marker for early endosomes, see Fig. S2). These results indicated that a fraction of cell-associated LCMV entered both early and late endosomes with a time course similar to that of the typical CME cargo SFV (Vonderheit and Helenius, 2005). At the time of onset of membrane fusion, the majority of viruses had reached late endosomes, which led us to conclude that LCMV penetration most likely occurred upon arrival in late, Rab7 and LAMP-1 containing endosomes.

Next, we compared the effect of DN Rab5 and Rab7 constructs on LCMV infection with the effects on SFV and SFV fus-1 (Fig. 8D). As expected, we found that SFV infection was partially inhibited by expression of the GDP-locked, constitutively inactive Rab5 S34N, but not by the corresponding Rab7 T22N construct (Sieczkarski and Whittaker, 2003). In contrast, SFV fus-1 infection was inhibited by Rab7 T22N (Fig. 8D). However, LCMV infection was reduced by 20% only in the Rab5 S34N expressing cells, and it was even less affected by Rab7 T22N, suggesting that only a minority population of the viruses depended on these endosomal GTPases for transport to the organelle of penetration.

The results raised the possibility that the major clathrin-independent pathway of LCMV internalization by-passed early endosomes altogether, and that the fraction of viruses found to colocalize with early endosomes corresponded to the minor fraction that entered through the clathrin-mediated pathway (Fig. 8C). Consistent with this, we did not observe significant colocalization of incoming LCMV with the early endosome marker EEA1 when CME was blocked by siRNA silencing of CHC in HeLa cells (Fig. 8E, solid lines). By comparing the colocalization time courses of LCMV with EEA1 and transferrin and by demonstrating that the virus did not enter transferrin-containing endosomes devoid of EEA1, we confirmed EEA1 was a reliable marker for the early endosomes that LCMV used after internalization via CME (Fig. S2).

However, trafficking of LCMV to LAMP-1-positive late endosomes occurred normally and with comparable kinetics in cells treated with anti-clathrin or control siRNA (Fig. 8F, solid vs. hatched lines). This strongly suggested that the fraction of LCMV virions internalized by the clathrin-independent route were indeed able to reach the late endosomes without passing through early endosomes.

Discussion

LCMV is known to belong to the acid-activated viruses (Borrow and Oldstone, 1994; Di Simone and Buchmeier, 1995; Di Simone et al., 1994), but how it enters cells and in which intracellular organelle the pH-induced membrane fusion occurs has remained unclear. Using immunofluorescence microscopy, we could demonstrate that LCMV-WE entered both early and late endosomes. The acid-dependent step occurred 10–20 min after warming coinciding with arrival of the virus in Rab7 and Lamp-1-positive late endosomes. The time course of entry is thus similar to that of influenza A virus and the fus-1 mutant of SFV, both of which are also thought to penetrate from late endosomes (Kielian et al., 1986; Sieczkarski and Whittaker, 2003). This was consistent with LCMV's pH threshold of 5.8 for *in vitro* fusion with liposomes and inactivation (Di Simone et al., 1994).

As schematically depicted in Fig. 9, our results indicated that LCMV-WE uses two pathways to reach the late endosomes. We estimate that about 20% of the incoming viruses are internalized via CME and delivered first to early endosomes and then to late endosomes. The rest make use of a novel clathrin-independent route that also delivers the viruses to late endosomes.

That a fraction of LCMV particles were internalized by CME was evident both from the EM images and from the small but consistent reduction in infection after silencing of clathrin heavy chain as well as expression of dominant-negative constructs of Eps15, Rab5a, and Rab7. The effects of dominant-negative constructs of Eps15 indicated that the viruses that entered via CME made use of clathrin-coated pits similar to those used by transferrin. In contrast, SFV, which was one of the control viruses used in our study, required clathrin but not Eps15. When clathrin heavy chains were silenced using siRNAs, incoming LCMV entered late endosomes but were no longer observed in early endosomes. Taken together, the data indicated that the LCMV particles internalized via CME were routed along the standard pathway via early endosomes to late endosomes, and that this involved both Rab5a and Rab7.

That the majority of viruses were internalized by a pathway independent of CME was demonstrated by electron microscopy; the majority of viruses were located in plasma membrane pits and cytoplasmic vesicles devoid of a clathrin coat. Also, LCMV infection was neither abolished by depletion of clathrin heavy chain nor by overexpression of dominant-negative constructs of dynamin-2, Eps15,

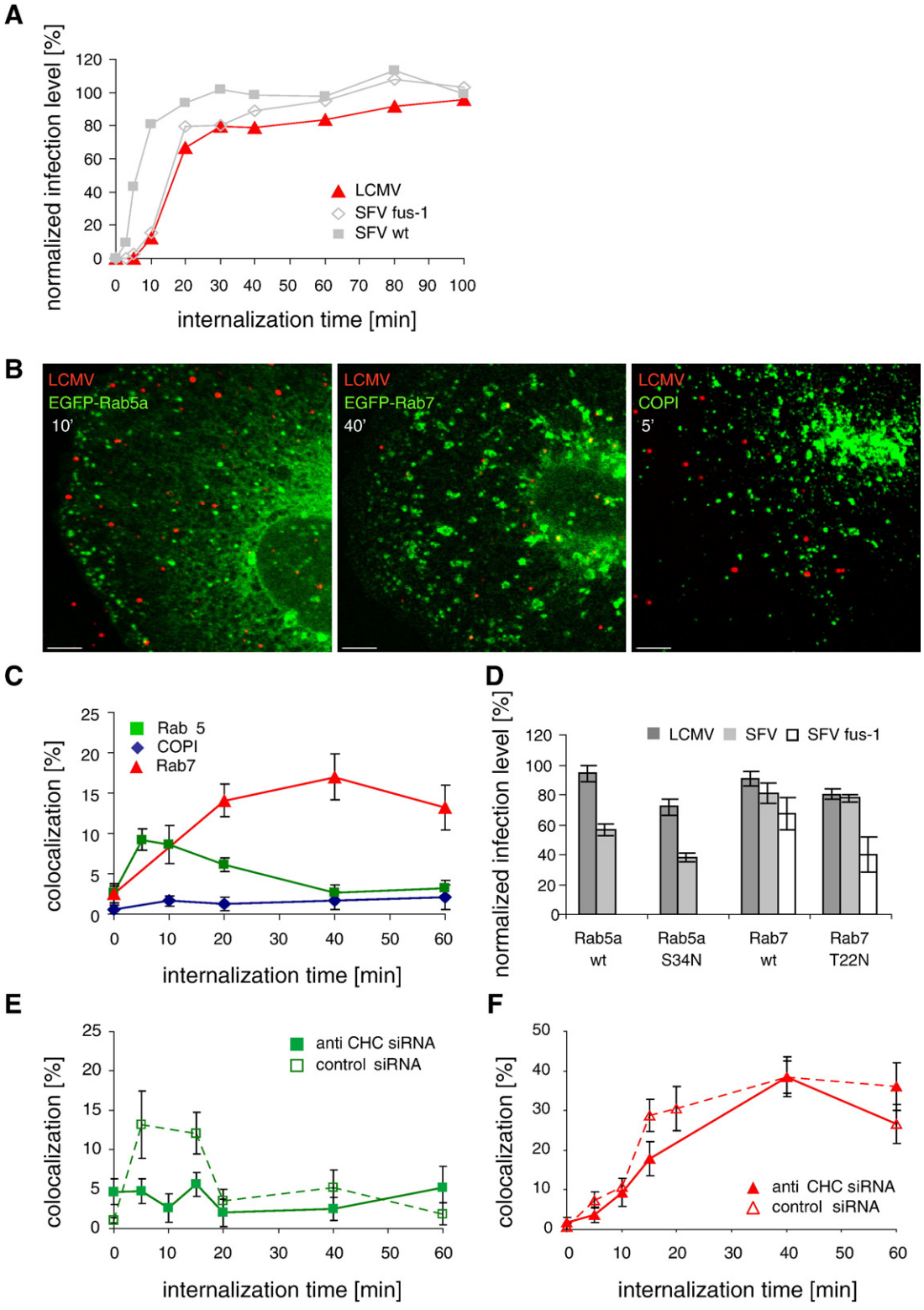

Fig. 8. Endosomal transport of LCMV. (A) Penetration time course of LCMV, SFV, and SFV fus-1 in Vero cells. The viruses (MOI = 0.2) were bound to cells on ice and then allowed to internalize after rapid warming to 37 °C for different times before addition of NH_4Cl containing medium to block further penetration and infection. The infection levels observed were normalized to the level in control cells. Error bars: SD of triplicate samples. (B) LCMV entry in Vero cells analyzed by confocal microscopy. Left: LCMV (red) and EGFP-Rab5 (green) at 10 min of internalization; middle: LCMV (red) and EGFP-Rab7 (green) at 40 min; right: LCMV (red) and COP I (green) at 5 min. (C) Quantification of colocalization with cellular markers. Per time point and marker, ca. 300 viruses in 7–10 cells were analyzed. Error bars: SE. (D) DN Rab5 and Rab7 reduce SFV or SFV fus-1 infection, but not LCMV infection. Infection was analyzed as in Fig. 2, the infection levels of transfected cells were normalized to the infection level of non-transfected cells in the same sample (MOI ~0.5 for all viruses). (E) Time course of colocalization with endogenous EEA1 in HeLa cells transfected with control siRNA or anti-CHC siRNA 1. (F) Time course of colocalization with endogenous LAMP-1 in HeLa cells transfected with control siRNA or anti-CHC siRNA. In panels E and F, only cells incapable to take up transferrin were analyzed for the CHC depleted samples. Per time point and marker, ca. 100 viruses in 10–15 cells were counted. Error bars: SE.

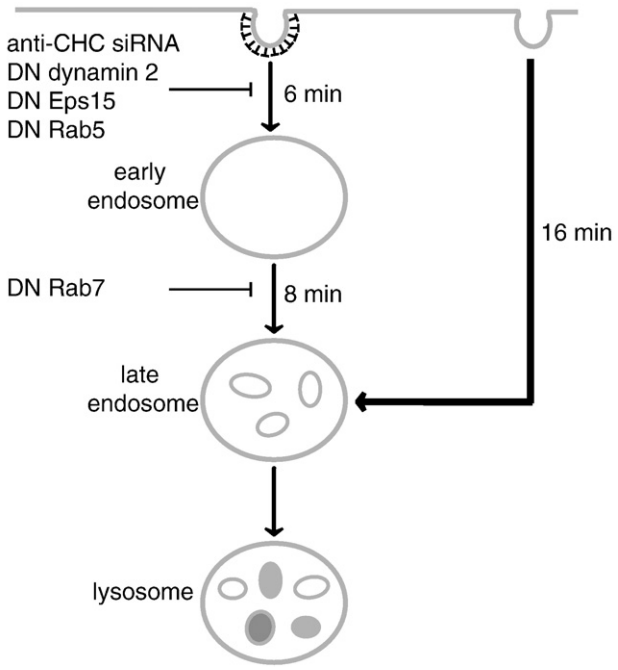

Fig. 9. Endocytic pathways exploited by LCMV. A minor fraction of LCMV enters cells via the classical CME pathway: these viruses are taken up and transported to early endosomes in a clathrin, dynamin-2, Eps15, and Rab5-dependent manner and depend on Rab7 for arrival at late endosomes. The major fraction of LCMV arrives in late endosomes with similar kinetics but makes use of a pathway that is independent on clathrin, dynamin-2, Eps15, Rab5, and Rab7. These viruses bypass classical early endosomes. This pathway is enhanced upon disruption of the cortical actin; it is independent of macropinocytosis, lipid rafts, Arf-6 and flotillin-1. Based on the effect of CME inhibitors in infection experiments performed at MOI 0.5, we roughly estimate that 80% of LCMV enters cells via the CME-independent pathway.

AP180, or Rab5a. The loss of incoming viruses that passed through EEA1-positive endosomes after silencing of clathrin heavy chain suggested that cargo in this pathway was delivered to late endosomes without passing through early endosomes.

The sensitivity of infection to different perturbations distinguished the major entry pathway from several clathrin-independent endocytic processes described for the uptake of viruses, toxins, endogenous ligands, and plasma membrane components (Mayor and Pagano, 2007). Infection was not affected by a dominant-negative dynamin-2 construct or by inhibitors of macropinocytosis. It was enhanced by disruption of the actin cytoskeleton, and perturbation of cholesterol in the plasma membrane indicated that functional lipid rafts were not required. Arf6 and flotillin-1 were, most likely, not involved.

This perturbation pattern was not consistent with any of the various pathways described in recent years, including (1) the caveolar pathway used by SV40 in CV-1 cells (Anderson et al., 1996); (2) the lipid raft and dynamin-dependent pathway used by the β-chain of interleukin-2 receptor, the γc cytokine receptor, autocrine motility factor, and echovirus 1 (Lamaze et al., 2001; Pietiainen et al., 2004; Sauvonnet et al., 2005); (3) the caveolin- and dynamin-independent, lipid-raft-dependent pathway used by SV40 particularly in cells devoid of caveolae (Damm et al., 2005); 4), the so-called GEEC pathway for the internalization of GPI-anchored proteins (Sabharanjak et al., 2002); and (5) the Arf6-dependent pathway for the internalization of class I MHC antigens (Naslavsky et al., 2004). In addition, we could eliminate macropinocytosis by the lack of F-actin dependence and the insensitivity to amiloride (Swanson and Watts, 1995). Further, since no colocalization between endogenous flotillin-1 and LCMV could be observed, the recently described flotillin-1-dependent pathway (Glebov et al., 2006; Payne et al., 2007) appeared not to be involved.

The lack of dependence on caveolin, Eps15, actin, and dynamin was very recently reported for entry of LCMV clone 13 into Vero E6 and CV1 cells (Rojek et al., 2007). The authors concluded like we did that the virus uses a novel endocytic pathway. In apparent contradiction to our results, but in agreement with another recent publication (Shah et al., 2006), they demonstrated that depletion of cholesterol inhibits LCMV internalization and infection. Both groups found a dose-dependent reduction in LCMV infection with 1–10 mM methyl-β-cyclodextrin, a drug that extracts cholesterol from the membrane rapidly and effectively. While this clearly demonstrated that LCMV entry depends on cholesterol, unambiguous conclusions about the involvement of lipid rafts and about the pathway of endocytosis cannot be made because, at the concentrations used, methyl-β-cyclodextrin may inhibit a variety of plasma membrane processes including CME (Martin-Acebes et al., 2007; Rodal et al., 1999; Subtil et al., 1999). Shah et al. (2006) also used a combination of progesterone, which inhibits cholesterol synthesis, and the cholesterol-sequestering agent nystatin (at a concentration 1000-fold higher than we did), and found partial inhibition of infection. When Kunz et al. employed nystatin and progesterone at a concentration 4-fold higher than ours, they found partial inhibition of LCMV clone 13 infection, an observation that we could confirm for LCMV-WE (Fig. S3). By contrast, when we adjusted the nystatin/progesterone concentrations to a lower level but sufficient to block the infection of the lipid-raft-dependent virus SV40 without effects on the entry of SFV (which does not require cholesterol for endocytosis via CME but requires cholesterol for membrane fusion in endosomes; Phalen and Kielian, 1991), we found that LCMV infection was not inhibited but, in fact, slightly enhanced. Barring effects due to differences in cell type and virus strain, one may conclude from the combined data that cholesterol is required for LCMV entry, but the type of lipid rafts involved in SV40 entry is not necessary for productive entry. The situation may resemble that found for type C food-and-mouth-disease virus, which needs cholesterol but does not depend an lipid rafts (for a discussion, see: Martin-Acebes et al., 2007). This possibility is consistent with the observations of Shah et al. (2006) that dystroglycan is not a lipid-raft-associated protein, and that it does not move into lipid rafts when associated with LCMV (Shah, Peng, and Carbonetto, 2006).

The clathrin-independent route taken by LCMV may share some properties with pathways used by the plant toxin ricin and by influenza A virus. Ricin binds to terminal galactose residues on glycolipids and glycoproteins and is internalized in cholesterol-depleted HeLa cells stably expressing dynamin-2 K44A (Rodal et al., 1999). However, due to its broad receptor spectrum, this lectin is endocytosed via virtually every pathway active in a given cell (Sandvig et al., 2002) making it difficult to define a single pathway without ambiguity. Influenza A entry and infection occurs in part by CME, but a considerable fraction of viruses seem to enter via smooth-walled structures whose morphology resembles those involved in LCMV internalization (Matlin et al., 1981). Influenza infects cholesterol-depleted cells expressing DN Eps15 (Sieczkarski and Whittaker, 2002), and live cell microscopy has revealed that a large fraction of the viruses enters without associating with detectable amounts of clathrin-EGFP (Rust et al., 2004). Although the alternative influenza entry pathway seems to have some features in common with LCMV entry, the dynamin-2, Rab5, and Rab7 dependence of influenza infection (Roy et al., 2000; Sieczkarski and Whittaker, 2003) suggests that the pathways are distinct. The examples of influenza virus and SV40 show that LCMV is not unique among viruses in having the capacity to use multiple pathways of endocytosis for entry. Such pleiotropy may provide an advantage for viruses by improving the chances for productive entry and broadening the cell specificity of infection.

The demonstration of yet another variant of clathrin-independent endocytosis in mammalian cells raises several questions to be answered in future work. Is the pathway used by LCMV also used for the internalization of physiological ligands and membrane

components or is it somehow induced by the virus particles? Which molecular machinery mediates vesicle formation, fission, transport, and targeting, and how is the pathway controlled? That the pathway seems to provide a direct connection from the plasma membrane to late endosomes is unique and may provide a clue as to a cellular function: the pathway may serve to internalize and down-regulate plasma membrane molecules and bound ligands that need to circumvent early endosomes to avoid recycling. By binding to the dystroglycan complex, LCMV and other arena viruses may have evolved to exploit a receptor, the internalization and turnover of which is controlled through this non-classical system. It is possible that Lassa fever virus, a highly pathogenic arenavirus, which unlike LCMV is strictly dependent on α-dystroglycan as a receptor, might rely exclusively on this novel endocytic mechanism. Future investigations with Arenaviridae and other viruses are likely to give exciting insights into the expanding repertoire of endocytic mechanisms and at the same time pave the way for the development of innovative anti-viral strategies.

Materials and methods

Cell culture and viruses

Vero and HeLa cells (both from ATCC) were maintained at 37 °C and 5% CO_2 in MEM medium supplemented with Earle's salts, GlutaMAXI, non-essential amino acids and 10% fetal calf serum. Infection of cells was carried out in R-medium, i.e., RPMI-1640 medium containing 0.2% bovine serum albumin, 10 mM HEPES/NaOH (pH 6.8), and Penicillin-Streptomycin. SFV wt, SFV fus-1, LCMV-WE, and SV40 were propagated and titers were determined according to standard protocols. A prototype tissue-culture-adapted SFV strain (SFV wt) and its mutant SFV fus-1 were grown in BHK-21 cells (Kääriäinen et al., 1969; Kielian et al., 1984). SV40 was propagated on CV-1 cells (Pelkmans et al., 2001). LCMV-WE was originally obtained from F. Lehmann-Grube (Heinrich Pette Institut, Hamburg, Germany) and was propagated in L-929 cells. This strain's GP sequence corresponds to the GP sequence AJ297484 of LCMV-WE54 (Beyer et al., 2001). Of note, LCMV-WE54 has been reported to strongly resemble LCMV clone 13 – the strain preferentially used in other studies on LCMV entry (Borrow and Oldstone, 1994; Rojek et al., 2007) – in terms of receptor binding characteristics, cellular tropism, and disease phenotype *in vivo* (Sevilla et al., 2000; Smelt et al., 2001; Kunz et al., 2004).

Antibodies and plasmids

The monoclonal antibodies VL-4 (rat) (Battegay et al., 1991) and KL-53 (mouse) (Zeller et al., 1988) against LCMV-NP were purified from hybridoma supernatant and directely labeled using NHS-activated Alexa Fluor 647 (Molecular Probes, Invitrogen Corporation). Mouse monoclonal antibody Pab 1605 against SV40 large T-antigen was obtained from G. Brandner (Freiburg). Polyclonal serum against SFV E1 and E2 was raised in rabbit (Singh and Helenius, 1992). Affinity-purified rabbit polyclonal anti-flotillin-1 antibody was kindly provided by K. Simons and had been raised against a flotillin-1 peptide. The mouse monoclonal antibodies KL-25 (Bruns et al., 1983), Wen-1, and Wen-4 (Seiler et al., 1998) against LCMV GP1 were purified from hybridoma supernatants. Anti-EEA1 and anti-clathrin heavy chain were from BD Transduction Laboratories, and anti-Lamp-1(clone H4A3) was from Santa Cruz Biotechnology; all secondary antibodies were bought from Molecular Probes (Invitrogen Corporation). Plasmids: human Eps15 Δ95/295-EGPF (Benmerah et al., 1999); human Eps15 DIIIΔ2-EGFP (Benmerah et al., 1998); rat dynamin2(aa)-EGFP and rat dynamin2(aa)K44A-EGFP (Cao et al., 2000); rat AP180 C-terminal domain-EGFP (Ford et al., 2001); pEGFP-Rab5a (Sonnichsen et al., 2000); Rab7-EGFP (Lebrand et al., 2002); and Arf6-EGFP (Naslavsky et al., 2004).

Transfection and siRNAs

For infection asssays, 2×10^5 Vero cells were plated on 4.5 cm^2 dishes and transfected ca. 16 h later using 2 μg plasmid DNA and 10 μl Superfect reagent (Qiagen). The cells were assayed 24 or 48 h (AP180) post-transfection. For immunofluorescence experiments, 10^6 exponentially growing Vero cells were transfected 5–7 h before with 2.5 μg plasmid DNA using the Amaxa Nucleofector, kit V, program A-24 (Amaxa, Köln, Germany). Anti-Luciferase (CGUACGCGGAAUACUUCGA), anti-CHC1 (CCUGCGGUCUGGAGUC AAC) (Hinrichsen et al., 2003), and anti-CHC2 (AUCCAAUUCGAAGACCAAU) (Motley et al., 2003) were from Qiagen. HeLa cells were transfected with siRNA using HiPerFect (Qiagen) essentially as described (Motley et al., 2003). After a first transfection at day 1, the cells were split the following day to maintain exponential growth, re-transfected at day 3, and split again at day 4. At day 5, infection or entry assays were carried out, and a parallel cell culture was lysed in SDS-loading buffer for SDS–PAGE and subsequent Western blot analysis.

Infection and transferrin uptake assays

The inoculum was prepared by diluting the appropriate amount of virus stock in R-medium (composition see above). Cells at 80% confluence were washed with R-medium, a small volume (500 μl per 4.5 cm^2, MOI ~0.5) of inoculum was added and the cells were incubated under normal growth conditions. A non-infected control was mock treated for later determination of the background signal. One hour p.i. (LCMV, SFV wt, SFV fus-1) or 2 h p.i. (SV40), the inoculum was replaced by normal growth medium. The cells were further incubated for until 5 h (SFV wt), 6 h (SFV fus-1), 12 h (LCMV), or 24 h (SV40) post-infection to allow synthesis of viral proteins. For FACS analysis, samples were trypsinized and fixed in 4% formaldehyde in PBS. The cells were resuspended in PBS containing 100 mM glycine and stored at 4 °C in the dark until staining (see below). Samples for microscopy were fixed for 10–15 min in 4% formaldehyde in DMEM buffered with 10 mM HEPES/NaOH pH 7, washed with PBS, and stored at 4 °C in the dark until staining. If an infection experiment was to be combined with a transferrin uptake assay, the cells were washed before fixation with DMEM and incubated for 10 min at 37 °C in DMEM containing 5 μg/ml fluorescently labeled transferrin (Molecular Probes, Invitrogen Corporation).

Pharmacological inhibitors

Nystatin (supplier: Sigma/solvent: DMSO/working concentration: 14, 7 μM) was combined with progesterone (Sigma/ethanol/16, 8 μM); amiloride (Calbiochem/DMSO/1, 20 μM); cytochalasin D (Calbiochem/DMSO/1, 20 μM); and jasplakinolide (Calbiochem/DMSO/50, 500 nM). Except for cholesterol depletion with nystatin/progesterone (7 h preincubation with the drugs in DMEM), the cells were preincubated with the inhibitors in R-medium for 45 min before infection. The inhibitors were present throughout the assay unless noted otherwise and did not affect cell viability. To probe their effect on the early steps of LCMV infection, the inhibitors were washed out 180 min post-infection using MEM supplemented with Earle's salts, GlutaMAXI, non-essential amino acids, 5% (v/v) fetal calf serum, 50 mM HEPES pH 7.6, and 20 mM ammonium chloride.

Penetration assays

Cells grown to 80% confluence were incubated on ice and washed with ice-cold R-medium. Ice-cold inoculum (MOI < 0.2) was added and the samples were incubated for 45 min on ice to allow binding of the virus. Unbound virus was washed off with ice-cold R-medium. The R-medium was replaced by normal growth medium containing 50 mM HEPES pH 7.6, and the samples were immediately transferred

to a 37 °C waterbath (t=0). At the times indicated, the medium was exchanged against normal growth medium containing 50 mM HEPES pH 7.6 and 20 mM ammonium chloride. Samples were harvested as described above.

Electron microscopy

Concentrated LCMV (10^8 pfu/ml) was bound to cells for 1 h on ice, unbound virus was removed, and PBS containing 10% FCS (PBS-10) was added. The cells were incubated on ice with antibodies against LCMV GP1 (20 μg/ml KL-25, 10 μg/ml Wen-1, 5 μg/ml Wen-4) for 1 h, washed in PBS-10, and incubated for 2 h with 10-nm gold-labeled goat anti-mouse antibodies on ice (Amersham Biosciences). The cells were washed with PBS-10 and transferred to a 37 °C water bath for 5, 10, or 30 min before fixation with 2% glutaraldehyde/2% osmium tetroxide and sample preparation according to standard EM protocols.

FACS analysis

To detect viral proteins, fixed cells were incubated in a dilution of the primary antibody in permeabilization solution (PBS containing 0.1% saponin, 20 mM EDTA, 0.02% sodium azide, and 2% FCS). LCMV-NP was stained using AlexaFluor 647-labeled VL-4 (20 μg/ml, 2 h at RT), SV40 large T-antigen was stained using Pab1605 (20 μg/ml, 2 h at RT), and SFV envelope proteins E1 and E2 were detected using rabbit polyclonal serum (1:100, 2 h at RT). The samples were washed 3 times in permeabilization solution and were stained with the appropriate secondary antibodies where needed (10 μg/ml, 2 h at RT). Sample analysis was performed on a FACS Calibur cytometer equipped with an FL-4 channel using CellQuest pro software (Becton Dickinson Immunocytometry Systems). For experiments with DN proteins, 50,000 cells per sample were counted, 2000–5000 of which strongly expressed the DN protein. For experiments with pharmacological inhibitors, 10 000 cells per sample were counted. Depending on the experiment, absolute infection levels between 20% and 70% were observed.

Entry assays, transferrin uptake, and immunofluorescence microscopy

To saturate intracellular compartments with transferrin, cells were washed once with DMEM, incubated for 10 min at 37 °C in DMEM containing 5 μg/ml fluorescently labeled transferrin (Molecular Probes, Invitrogen Corporation) and transferred to ice. LCMV (MOI ~50) was bound to cells on ice for 1 h, unbound virus was removed by washing once with R-medium, R-medium containing 5 μg/ml fluorescently labeled transferrin was added, and the samples were shifted to a 37° water bath to allow endocytosis of LCMV and transferrin. After varying times at 37 °C, the samples were fixed in 4% formaldehyde in DMEM buffered with 10 mM HEPES/NaOH pH 7 for 15 min at RT and washed in PBS. Cells were permeabilized in PBS containing 0.05% saponin, 10% goat serum and 5% FCS, and LCMV was stained over night at 4 °C using VL-4 (5 μg/ml) followed by an appropriate goat anti-rat secondary antibody. For co-stainings with mouse monoclonal antibodies, the cells were first incubated with the mouse antibody followed by a goat anti-mouse secondary antibody. The samples were then fixed in 4% formaldehyde in PBS, residual formaldehyde was quenched by washing in PBS containing 100 mM glycine, and LCMV was stained over night at 4 °C using directly labeled VL-4 (20 μg/ml) and KL-53 (20 μg/ml). After washing, the samples were mounted on microscopy slides using Shandon Immu-Mount (Thermo Electron, Dreieich, Germany). Microscopy was performed at room temperature using an inverted Zeiss laser scanning confocal microscope (model 510Meta, Carl Zeiss MicroImaging, Inc.) equipped with a 100× Zeiss apochomat objective (1.4 NA) and an Argon laser (458, 477, 488, 514) 30 mW, HeNe laser (543 nm) 1 mW, or HeNe laser (633 nm) 5 mW. All samples within one experiment were acquired with the same microscope settings using the LSM 510 software package (Carl Zeiss MicroImaging, Inc.). Both LCMV staining protocols resulted in no background signal at all if LCMV was omitted from the samples. Images were processed using Adobe Photoshop for cropping and slight adjustments of intensity.

Colocalization analysis

Viruses were considered for analysis only if their apparent size was between 0.5- and 1.2-fold of the calculated diameter of the airy disk. A virus was considered to colocalize with a given marker if at least 50% of the virus overlapped with the marker and if the maker signal exhibited at the same time a clear local maximum below the virus.

Acknowledgments

We thank G. Brandner, A. Dautry-Varsat, H. McMahon, M. McNiven, J. Gruenberg, K. Simons, and M. Zerial for gifts of reagents. H. Hengartner and R. Zinkernagel provided us with LCMV-WE and generously shared their expertise on LCMV. L. Diener and R. Mancini helped to prepare the electron microscopy samples. Thanks to F. Thor, S. Moese, and A. Hayer for critical reading of the manuscript. This work was supported by the Swiss National Science Foundation and by grant TH-16/04-1 from ETH Zurich.

Appendix A. Supplementary data

Supplementary data associated with this article can be found, in the online version, at doi:10.1016/j.virol.2008.04.046.

References

Anderson, H.A., Chen, Y., Norkin, L.C., 1996. Bound simian virus 40 translocates to caveolin-enriched membrane domains, and its entry is inhibited by drugs that selectively disrupt caveolae. Mol. Biol. Cell 7 (11), 1825–1834.
Barton, L.L., Mets, M.B., 2001. Congenital lymphocytic choriomeningitis virus infection: decade of rediscovery. Clin. Infect. Dis. 33 (3), 370–374.
Battegay, M., Cooper, S., Althage, A., Banziger, J., Hengartner, H., Zinkernagel, R.M., 1991. Quantification of lymphocytic choriomeningitis virus with an immunological focus assay in 24- or 96-well plates. J. Virol. Methods 33 (1–2), 191–198.
Benmerah, A., Bayrou, M., Cerf-Bensussan, N., Dautry-Varsat, A., 1999. Inhibition of clathrin-coated pit assembly by an Eps15 mutant. J. Cell Sci. 112 (Pt 9), 1303–1311.
Benmerah, A., Lamaze, C., Begue, B., Schmid, S.L., Dautry-Varsat, A., Cerf-Bensussan, N., 1998. AP-2/Eps15 interaction is required for receptor-mediated endocytosis. J. Cell Sci. 140 (5), 1055–1062.
Beyer, W.R., Miletic, H., Ostertag, W., von Laer, D., 2001. Recombinant expression of lymphocytic choriomeningitis virus strain we glycoproteins: a single amino acid makes the difference. J. Virol. 75 (2), 1061–1064.
Borrow, P., Oldstone, M.B., 1994. Mechanism of lymphocytic choriomeningitis virus entry into cells. Virology 198 (1), 1–9.
Bruns, M., Martinez Peralta, L., Lehmann-Grube, F., 1983. Lymphocytic choriomeningitis virus. III. Structural proteins of the virion. J. Gen. Virol. 64 (Pt 3), 599–611.
Buchmeier, M.J., 2002. Arenaviruses: protein structure and function. Curr. Top. Microbiol. Immunol. 262, 159–173.
Cao, H., Thompson, H.M., Krueger, E.W., McNiven, M.A., 2000. Disruption of Golgi structure and function in mammalian cells expressing a mutant dynamin. J. Cell Sci. 113 (11), 1993–2002.
Cao, W., Henry, M.D., Borrow, P., Yamada, H., Elder, J.H., Ravkov, E.V., Nichol, S.T., Compans, R.W., Campbell, K.P., Oldstone, M.B., 1998. Identification of alpha-dystroglycan as a receptor for lymphocytic choriomeningitis virus and Lassa fever virus. Science 282 (5396), 2079–2081.
Charrel, R.N., Lamballerie, X.d., 2003. Arenaviruses other than Lassa virus. Antivir. Res. 57 (1–2), 89–100.
Conner, S.D., Schmid, S.L., 2003. Differential requirements for AP-2 in clathrin-mediated endocytosis. J. Cell Sci. 162 (5), 773–779.
D'Souza-Schorey, C., Chavrier, P., 2006. ARF proteins: roles in membrane traffic and beyond. Nat. Rev., Mol. Cell Biol. 7 (5), 347–358.
Damm, E.-M., Pelkmans, L., Kartenbeck, J., Mezzacasa, A., Kurzchalia, T., Helenius, A., 2005. Clathrin- and caveolin-1-independent endocytosis: entry of simian virus 40 into cells devoid of caveolae. J. Cell Sci. 168 (3), 477–488.
Di Simone, C., Buchmeier, M.J., 1995. Kinetics and pH dependence of acid-induced structural changes in the lymphocytic choriomeningitis virus glycoprotein complex. Virology 209 (1), 3–9.
Di Simone, C., Zandonatti, M.A., Buchmeier, M.J., 1994. Acidic pH triggers LCMV membrane fusion activity and conformational change in the glycoprotein spike. Virology 198 (2), 455–465.
Donaldson, J.G., 2003. Multiple roles for Arf6: sorting, structuring, and signaling at the plasma membrane. J. Biol. Chem. 278 (43), 41573–41576.

Eschli, B., Quirin, K., Wepf, A., Weber, J., Zinkernagel, R., Hengartner, H., 2006. Identification of an N-terminal trimeric coiled-coil core within Arenavirus glycoprotein 2 permits assignment to class I viral fusion proteins. J. Virol. 80 (12), 5897–5907.

Ford, M.G., Pearse, B.M., Higgins, M.K., Vallis, Y., Owen, D.J., Gibson, A., Hopkins, C.R., Evans, P.R., McMahon, H.T., 2001. Simultaneous binding of PtdIns(4,5)P2 and clathrin by AP180 in the nucleation of clathrin lattices on membranes. Science 291 (5506), 1051–1055.

Glebov, O.O., Bright, N.A., Nichols, B.J., 2006. Flotillin-1 defines a clathrin-independent endocytic pathway in mammalian cells. Nat. Cell Biol. 8 (1), 46–54.

Helenius, A., Kartenbeck, J., Simons, K., Fries, E., 1980. On the entry of Semliki Forest virus into BHK-21 cells. J. Cell Sci. 84 (2), 404–420.

Hinrichsen, L., Harborth, J., Andrees, L., Weber, K., Ungewickell, E.J., 2003. Effect of clathrin heavy chain- and alpha-adaptin-specific small inhibitory RNAs on endocytic accessory proteins and receptor trafficking in HeLa cells. J. Biol. Chem. 278 (46), 45160–45170.

Imperiali, M., Thoma, C., Pavoni, E., Brancaccio, A., Callewaert, N., Oxenius, A., 2005. O Mannosylation of {alpha}-dystroglycan is essential for lymphocytic choriomeningitis virus receptor function. J. Virol. 79 (22), 14297–14308.

Kääriäinen, L., Simons, K., von Bonsdorff, C.H., 1969. Studies in subviral components of Semliki Forest virus. Ann. Med. Exp. Biol. Fenn. 47 (4), 235–248.

Kielian, M.C., Keranen, S., Kaariainen, L., Helenius, A., 1984. Membrane fusion mutants of Semliki Forest virus. J. Cell Sci. 98 (1), 139–145.

Kielian, M.C., Marsh, M., Helenius, A., 1986. Kinetics of endosome acidification detected by mutant and wild-type Semliki Forest virus. EMBO J. 5 (12), 3103–3109.

Krauss, M., Kinuta, M., Wenk, M.R., De Camilli, P., Takei, K., Haucke, V., 2003. ARF6 stimulates clathrin/AP-2 recruitment to synaptic membranes by activating phosphatidylinositol phosphate kinase type I{gamma}. J. Cell Sci. 162 (1), 113–124.

Kunz, S., Sevilla, N., Rojek, J.M., Oldstone, M.B.A., 2004. Use of alternative receptors different than [alpha]-dystroglycan by selected isolates of lymphocytic choriomeningitis virus. Virology 325 (2), 432–445.

Kunz, S., Rojek, J.M., Kanagawa, M., Spiropoulou, C.F., Barresi, R., Campbell, K.P., Oldstone, M.B.A., 2005. Posttranslational modification of {alpha}-dystroglycan, the cellular receptor for Arenaviruses, by the glycosyltransferase LARGE is critical for virus binding. J. Virol. 79 (22), 14282–14296.

Lakadamyali, M., Rust, M.J., Zhuang, X., 2006. Ligands for clathrin-mediated endocytosis are differentially sorted into distinct populations of early endosomes. Cell 124 (5), 997–1009.

Lamaze, C., Dujeancourt, A., Baba, T., Lo, C.G., Benmerah, A., Dautry-Varsat, A., 2001. Interleukin 2 receptors and detergent-resistant membrane domains define a clathrin-independent endocytic pathway. Mol. Cell 7 (3), 661–671.

Lebrand, C., Corti, M., Goodson, H., Cosson, P., Cavalli, V., Mayran, N., Faure, J., Gruenberg, J., 2002. Late endosome motility depends on lipids via the small GTPase Rab7. EMBO J. 21 (6), 1289–1300.

Marsh, M., Helenius, A., 2006. Virus entry: open sesame. Cell 124 (4), 729–740.

Martin-Acebes, M.A., Gonzalez-Magaldi, M., Sandvig, K., Sobrino, F., Armas-Portela, R., 2007. Productive entry of type C foot-and-mouth disease virus into susceptible cultured cells requires clathrin and is dependent on the presence of plasma membrane cholesterol. Virology 369 (1), 105–118.

Matlin, K.S., Reggio, H., Helenius, A., Simons, K., 1981. Infectious entry pathway of influenza virus in a canine kidney cell line. J. Cell Sci. 91 (3 Pt 1), 601–613.

Mayor, S., Pagano, R.E., 2007. Pathways of clathrin-independent endocytosis. Nat. Rev., Mol. Cell Biol. 8 (8), 603–612.

Meyerholz, A., Hinrichsen, L., Groos, S., Esk, P.-C., Brandes, G., Ungewickell, E.J., 2005. Effect of clathrin assembly lymphoid myeloid leukemia protein depletion on clathrin coat formation. Traffic 6 (12), 1225–1234.

Motley, A., Bright, N.A., Seaman, M.N., Robinson, M.S., 2003. Clathrin-mediated endocytosis in AP-2-depleted cells. J. Cell Sci. 162 (5), 909–918.

Naslavsky, N., Weigert, R., Donaldson, J.G., 2003. Convergence of non-clathrin- and clathrin-derived endosomes involves Arf6 inactivation and changes in phosphoinositides. Mol. Biol. Cell 14 (2), 417–431.

Naslavsky, N., Weigert, R., Donaldson, J.G., 2004. Characterization of a nonclathrin endocytic pathway: membrane cargo and lipid requirements. Mol. Biol. Cell 15 (8), 3542–3552.

Neuman, B.W., Adair, B.D., Burns, J.W., Milligan, R.A., Buchmeier, M.J., Yeager, M., 2005. Complementarity in the supramolecular design of arenaviruses and retroviruses revealed by electron cryomicroscopy and image analysis. J. Virol. 79 (6), 3822–3830.

Oh, P., McIntosh, D.P., Schnitzer, J.E., 1998. Dynamin at the neck of caveolae mediates their budding to form transport vesicles by GTP-driven fission from the plasma membrane of endothelium. J. Cell Sci. 141 (1), 101–114.

Ohkuma, S., Poole, B., 1978. Fluorescence probe measurement of the intralysosomal pH in living cells and the perturbation of pH by various agents. Proc. Natl. Aca. Sci. U. S. A. 75, 3327–3331.

Paleotti, O., Macia, E., Luton, F., Klein, S., Partisani, M., Chardin, P., Kirchhausen, T., Franco, M., 2005. The small G-protein Arf6GTP recruits the AP-2 adaptor complex to membranes. J. Biol. Chem. 280 (22), 21661–21666.

Parton, R.G., Richards, A.A., 2003. Lipid rafts and caveolae as portals for endocytosis: new insights and common mechanisms. Traffic 4 (11), 724–738.

Payne, C.K., Jones, S.A., Chen, C., Zhuang, X., 2007. Internalization and trafficking of cell surface proteoglycans and proteoglycan-binding ligands. Traffic 8 (4), 389–401.

Pelkmans, L., Kartenbeck, J., Helenius, A., 2001. Caveolar endocytosis of simian virus 40 reveals a new two-step vesicular-transport pathway to the ER. Nat. Cell Biol. 3 (5), 473–483.

Pelkmans, L., Puntener, D., Helenius, A., 2002. Local actin polymerization and dynamin recruitment in SV40-induced internalization of caveolae. Science 296 (5567), 535–539.

Peters, C.J., 2006. Lymphocytic choriomeningitis virus–an old enemy up to new tricks. N. Engl. J. Med. 354 (21), 2208–2211.

Phalen, T., Kielian, M., 1991. Cholesterol is required for infection by Semliki Forest virus. J. Cell Sci. 112 (4), 615–623.

Pietiainen, V., Marjomaki, V., Upla, P., Pelkmans, L., Helenius, A., Hyypia, T., 2004. Echovirus 1 endocytosis into caveosomes requires lipid rafts, dynamin II, and signaling events. Mol. Biol. Cell 15 (11), 4911–4925.

Rodal, S.K., Skretting, G., Garred, O., Vilhardt, F., van Deurs, B., Sandvig, K., 1999. Extraction of cholesterol with methyl-beta-cyclodextrin perturbs formation of clathrin-coated endocytic vesicles. Mol. Biol. Cell 10 (4), 961–974.

Rojek, J.M., Perez, M., Kunz, S., 2007. Cellular entry of lymphocytic choriomeningitis Virus. J. Virol. JVI.0149331-07.

Roy, A.M., Parker, J.S., Parrish, C.R., Whittaker, G.R., 2000. Early stages of influenza virus entry into Mv-1 lung cells: involvement of dynamin. Virology 267 (1), 17–28.

Rust, M.J., Lakadamyali, M., Zhang, F., Zhuang, X., 2004. Assembly of endocytic machinery around individual influenza viruses during viral entry. Nat. Struct. Mol. Biol. 11 (6), 567–573.

Sabharanjak, S., Sharma, P., Parton, R.G., Mayor, S., 2002. GPI-anchored proteins are delivered to recycling endosomes via a distinct cdc42-regulated, clathrin-independent pinocytic pathway. Dev. Cell. 2 (4), 411–423.

Sandvig, K., Grimmer, S., Lauvrak, S., Torgersen, M., Skretting, G., van Deurs, B., Iversen, T., 2002. Pathways followed by ricin and Shiga toxin into cells. Histochem. Cell Biol. 117 (2), 131–141.

Sauvonnet, N., Dujeancourt, A., Dautry-Varsat, A., 2005. Cortactin and dynamin are required for the clathrin-independent endocytosis of {gamma}c cytokine receptor. J. Cell Sci. 168 (1), 155–163.

Seiler, P., Kalinke, U., Rulicke, T., Bucher, E.M., Bose, C., Zinkernagel, R.M., Hengartner, H., 1998. Enhanced virus clearance by early inducible lymphocytic choriomeningitis virus-neutralizing antibodies in immunoglobulin-transgenic mice. J. Virol. 72 (3), 2253–2258.

Sevilla, N., Kunz, S., Holz, A., Lewicki, H., Homann, D., Yamada, H., Campbell, K.P., de la Torre, J.C., Oldstone, M.B.A., 2000. Immunosuppression and resultant viral persistence by specific viral targeting of dendritic cells. J. Exp. Med. 192 (9), 1249–1260.

Shah, W.A., Peng, H., Carbonetto, S., 2006. Role of non-raft cholesterol in lymphocytic choriomeningitis virus infection via {alpha}-dystroglycan. J. Gen. Virol. 87 (3), 673–678.

Sieczkarski, S.B., Whittaker, G.R., 2002. Influenza virus can enter and infect cells in the absence of clathrin-mediated endocytosis. J. Virol. 76 (20), 10455–10464.

Sieczkarski, S.B., Whittaker, G.R., 2003. Differential requirements of Rab5 and Rab7 for endocytosis of influenza and other enveloped viruses. Traffic 4 (5), 333–343.

Singh, I., Helenius, A., 1992. Role of ribosomes in Semliki Forest virus nucleocapsid uncoating. J. Virol. 66 (12), 7049–7058.

Smelt, S.C., Borrow, P., Kunz, S., Cao, W., Tishon, A., Lewicki, H., Campbell, K.P., Oldstone, M.B.A., 2001. Differences in affinity of binding of lymphocytic choriomeningitis virus strains to the cellular receptor {alpha}-dystroglycan correlate with viral tropism and disease kinetics. J. Virol. 75 (1), 448–457.

Sonnichsen, B., De Renzis, S., Nielsen, E., Rietdorf, J., Zerial, M., 2000. Distinct membrane domains on endosomes in the recycling pathway visualized by multicolor imaging of Rab4, Rab5, and Rab11. J. Cell Sci. 149 (4), 901–914.

Subtil, A., Gaidarov, I., Kobylarz, K., Lampson, M.A., Keen, J.H., McGraw, T.E., 1999. Acute cholesterol depletion inhibits clathrin-coated pit budding. Proc. Natl. Acad. Sci. U. S. A. 96 (12), 6775–6780.

Swanson, J.A., Watts, C., 1995. Macropinocytosis. Trends Cell Biol. 5 (11), 424–428.

Tebar, F., Bohlander, S.K., Sorkin, A., 1999. Clathrin assembly lymphoid myeloid leukemia (CALM) protein: localization in endocytic-coated pits, interactions with clathrin, and the impact of overexpression on clathrin-mediated traffic. Mol. Biol. Cell 10 (8), 2687–2702.

van der Bliek, A.M., Redelmeier, T.E., Damke, H., Tisdale, E.J., Meyerowitz, E.M., Schmid, S.L., 1993. Mutations in human dynamin block an intermediate stage in coated vesicle formation. J. Cell Sci. 122 (3), 553–563.

Vonderheit, A., Helenius, A., 2005. Rab7 associates with early endosomes to mediate sorting and transport of semliki forest virus to late endosomes. PLoS Biol. 3 (7).

Zeller, W., Bruns, M., Lehmann-Grube, F., 1988. Lymphocytic choriomeningitis virus X. Demonstration of nucleoprotein on the surface of infected cells. Virology 162 (1), 90–97.